Title: Monitoring the physical state of wood during multiple tensile load-unload cycles by the eigenvalue distribution of near infrared spectra

Type of article: Original research papers

Author name and affiliation:

Takaaki Fujimoto * Corresponding author

Faculty of Agriculture, Tottori University, Tottori, 680-8553, Japan

Tel. and Fax: +81-857-31-5866; E-mail: tafujimoto@tottori-u.ac.jp

Abstract

Wood is a typical viscoelastic material that shows a clear mechanical hysteresis loop during cyclic loading, which implies the irreversibility of the process and is important for the processing and long-term utility of wood. We examined the changes in the physical state of wood during multiple tensile load-unload cycles based on the eigenvalue distribution of the near-infrared spectra. The set of eigenvalues $H = \{\lambda_1, \lambda_2, \ldots, \lambda_n\}$, calculated from the spectral matrix successively acquired during the cycling test, was treated as the Hamiltonian, which represents the energy eigenstate of the wood. Using statistical physics and random matrix theory, the variation in the physical state of wood was discussed from both macroscopic and microscopic perspectives. Unlike traditional methods, the energy state of wood can be followed in real time during cyclic loading; in other words, the Helmholtz free energy and Shannon entropy varied with load changes. The commutator, defined by the density and diagonal matrix of H, could be used to quantitatively evaluate the irreversible changes in wood during the cyclic processes. The proposed method is independent of a specific coordinate system, and can therefore be applied using a wide variety of chemical information other than that obtained from the near-infrared spectra.

Keywords: Symmetry breakage; Cellulose crystallinity; Helmholtz free energy; Entropy; Liouville-von Neumann equation.

1. Introduction

Repeated cycles, such as adsorption-desorption of moisture and removal of load, are inevitable when using wood for extended periods. To understand how wood undergoes changes in such repeated processes is of particular interest. For example, the effects of repeated wetting and drying cycles on the physical and mechanical properties of thermally modified wood and wood-plastic composites have been extensively studied.[1–3] In addition, cyclic loadings, assuming long-term use of wood, have been investigated to elucidate the lifetime of wood products, such as furniture and construction components.[4–6] On a larger timescale, these discussions have evolved to studies of archaeological timber.[7–9] Moreover, detailed examinations of cell wall components have been extended to the microscopic level.[10–13]

A notable phenomenon in the cyclic process of wood is hysteresis.[4,14] For example, during cyclic changes in relative humidity, the path of moisture in the drying process is clearly different from that in the wetting process.[15,16] In addition, wood never returns to its original state strictly at the end of a cycle, indicating that it changed irreversibly. Therefore, the physical state of harvested green wood changes constantly with time.[17] This irreversible change can be macroscopically recognized as a permanent deformation during the loading-unloading cycle. The area surrounded by the paths indicate the energy loss of the system during the cycle.[4] Although irreversible

48 changes at the molecular level have been examined[10,12], the relationship between the
49 macroscopic and microscopic properties remain unclear. This study discusses the
50 changes in the state of wood under irreversible processes, both macroscopically and
51 microscopically, based on statistical physics coupled with random matrix theory.

52 Considering that a given wood can be characterized by various properties, such as
53 wood density, mechanical properties, chemical components, and anatomical features,
54 changes in one property can induce corresponding changes in many other properties.[18]
55 For example, when monitoring the load changes during the load-unload cycles, other
56 properties, such as the configuration of molecules in the cell wall, are expected to
57 change as a result of such changes. In this regard, the irreversibility of wood in cyclic
58 processes is not difficult to visualize because wood is a highly heterogeneous
59 composite material consisting of three major natural polymers. Therefore, we
60 evaluated the change in multiple characteristics with respect to others to comprehend
61 the physical state of wood at every moment.

62 Fujimoto et al. proposed a method based on the distribution of eigenvalues to
63 comprehensively evaluate the change in multiple wood characteristics.[19–22] In this
64 method, the multi-dimensional data obtained from wood were identified as state
65 vectors, representing the physical characteristics of the system. A matrix composed of
66 several state vectors can be classified as an operator representing the physical quantity

of the statistical ensemble.[23] The eigenvalues calculated from the matrix must reflect every interrelation between the numerous properties of wood. Moreover, the set of eigenvalues represents the energy state of the system in the context of physics[24–27]; thus, changes in wood can be analyzed from the perspective of thermodynamics and statistical mechanics.[28–30] The eigenvalue distribution at each point in time was calculated during the stress relaxation test, which was used to quantitatively evaluate the time dependencies of the Helmholtz free energy and entropy.[20]

A notable point of this method is that *n*-dimensional data from wood do not necessarily have to exhibit a one-to-one correspondence with the wood properties. This is supported by many previous studies that have estimated various wood properties with indirect information, such as near infrared (NIR) spectra and acoustic spectra.[31–34] As the statistical model obtained in these studies is a covector[35], the idea is also supported by the mathematical concept of duality. This indirect manner of evaluating the actual variation in wood properties comprehensively provides great advantages and is consistent with one of the characteristic features of the analytical mechanics, in which the nature of the coordinates that translate a given physical situation into an abstract mathematical situation is not specified.[36,37] Moreover, the characteristic equation to solve the eigenvalue problem is invariant with respect to changes in the basis.[38] Therefore, the set of eigenvalues reveals the intrinsic variation of the wood

ensemble.

In this study, we investigated changes in the physical state of wood under multiple tensile load-unload cycles based on the eigenvalue analysis of near-infrared spectral matrices. Unlike traditional procedures, this method can be used to quantitatively evaluate the energy state at each point in time. From a geometric perspective, wood characterized by n variables can be defined as a point in the n-dimensional real number space $\mathbb{R}^n$ to be an n-tuple of numbers (x_1, x_2, ..., x_n), where n is a positive integer[19]; in other words, we can identify the changes in wood under cyclic processes as the motion of the mass point in the configuration space.[36,37] The symmetry of the process is discussed based on this geometrical picture.

2. Material and methods

2.1. Sample preparation

The samples were prepared according to previously reported procedures[19–22]: Twenty blocks of dimensions 20 mm (radial) × 20 mm (tangential) × 50 mm (longitudinal) were cut from the logs of 20 50-year-old Japanese larch (*Larix kaempferi*) trees. The blocks were selected to have a wide range of variation in the Young's modulus. Several thin sections (thickness = 200 μm) per block were sliced from the radial-longitudinal surface using a microtome. All the sections were conditioned to equilibrium in a thermo-hygrostat (LH-114, ESPEC Co., Osaka, Japan) maintained at

105 20 °C and 60% relative humidity. The average moisture content of the sections in the
106 subsequent test was approximately 12%.

107 **2.2. Mechanical test**

108 Prior to the cyclic tensile test, the destructive test was conducted parallel to the
109 grain using a thin section corresponding to each sample block. The load was applied
110 along the longitudinal direction at a rate of 0.01 mm/min and the deflection was
111 measured by crosshead movements. The load and deflection data were recorded at 1 s
112 intervals using a data logger (NR-500, KEYENCE Co., Osaka, Japan).

113 Cyclic loading was performed for the one-sided tests[4]; in other words, uniaxial
114 tensile loads along the longitudinal direction were applied such that the magnitude
115 increases to some pre-determined level and returns to zero during a complete cycle.
116 The ultimate load of the cycle was constantly set at 50% of the maximum load
117 obtained from the destructive test. The load and unload rates were the same as those in
118 the destructive test. The cycle test was repeated five times and conducted at room
119 temperature (~25 °C and 60% relative humidity).

120 **2.3. NIR measurement**

121 Diffuse reflectance spectra were acquired using a Fourier-transform infrared
122 spectrophotometer (MATRIX-F, Bruker Optics Co., Tokyo, Japan) equipped with a
123 fiber-optic probe (spot diameter ≈ 3.5 mm). The probe was positioned on the

124 radial-longitudinal phase of the section, and the spectra were obtained at intervals of 8
125 cm^{-1} over the wavenumber range of 10000–4000 cm^{-1}. Zero-filling of two,
126 corresponding to a spectral interval of 4 cm^{-1}, was applied. Thirty-two scans were
127 collected to improve the signal-to-noise ratio and averaged into a single average
128 spectrum. We obtained a single spectrum after approximately 10 s under these
129 conditions. The number of measurement points per half cycle were fixed at six for each
130 sample; namely, the same position was repeatedly measured 6 times. Therefore, the
131 total number of measurements over five cycles were 60.

132 The following analyses focused on the wavenumber range of 9000–4500 cm^{-1} to
133 reduce the computational complexity.[19–21] The original spectra were processed vector
134 normalization prior to the spectral analyses. A total of 1168 data points were used as
135 spectral variables across the spectral range of 9000–4500 cm^{-1}.

136 **2.4. Data analysis**

137 The 20 × 1168 spectral matrix $\boldsymbol{A}$ was obtained at each measurement point in time
138 t_1, t_2, …, t_{60}. An eigenvalue decomposition was applied to the variance–covariance
139 matrix $\boldsymbol{C}$ calculated from the spectral matrix $\boldsymbol{A}$ ($\boldsymbol{C} = \boldsymbol{A}^{\mathrm{T}}\boldsymbol{A}$). The eigenvalue problem
140 was solved by maximizing the quadratic form $\boldsymbol{u}^{\mathrm{T}}_i\boldsymbol{C}\boldsymbol{u}_i$ with respect to the eigenvector $\boldsymbol{u}_i$
141 ($i = 1,\cdots, N$).[26,39] The set of eigenvalues $\{\lambda_1, \lambda_2, \ldots, \lambda_N\}$ was considered to belong to an
142 energy function, termed the Hamiltonian H.[23–27] Once H is defined, the distribution

function Z can be calculated as follows[28–30]:

$$Z = \sum_{i=1}^{N} \exp(-\beta\lambda_i) \quad (1)$$

where β is the inverse temperature defined as $\beta = (kT)^{-1}$ (k represents the Boltzmann constant and T is the absolute temperature). Thermodynamic functions, such as the Helmholtz free energy and entropy, can be obtained from the distribution function, as mentioned below. Based on the time evolution of these thermodynamic functions, we discuss the macroscopic and microscopic changes in the energy state of wood during the cyclic process. These calculations were performed using the standard functions of R version 3.6.1.

3. Results and discussion

3.1. Cyclic tensile test

Figure 1 shows the load-displacement curve during the cyclic tensile test. Because wood is a typical viscoelastic material, the cycle exhibited a clear mechanical hysteresis loop. For example, the gap between the loading and unloading paths at a load level of 60 N was approximately 30% in the first cycle, indicating a significant delay in displacement during unloading. The path and residual displacement delays were greatest in the first cycle and decreased after the second cycle. The slope of the loading curve increased from the first to the second cycle and remained high thereafter.

160 One of the causes of these results may be the microfractures that formed by clamping
161 the specimen. These results are frequently observed in cyclic tests.

162 In the traditional method, the energy that is lost during the load-unload cycle is
163 evaluated by the area of the hysteresis loop.[4,40,41] The ratio of lost to stored energy (i.e.,
164 energy recovered through elastic contraction of the specimen) is referred to as tan δ in
165 the dynamic mechanical analysis. Alternatively, this study attempted to monitor the
166 changes in the energy state of wood at each point in time based on the eigenvalue
167 distribution from the NIR spectral matrix. Indeed, the area of the hysteresis loop shown
168 the similar tendency with the Helmholtz free energy (Figure 4(a)).

169 **3.2. Variation of NIR spectra**

170 Figure 2 shows the variation in the NIR spectra acquired during the loading and
171 unloading process for a representative sample. The absorbance intensity in the entire
172 wavenumber range gradually increased with load (the color of the spectra changes
173 from yellow to red, as shown in Fig. 2(a)) and subsequently decreased with unloading
174 (the color of the spectra changes from yellow to blue, as shown in Fig. 2(b)). The
175 second derivative spectra (data not shown) emphasized the variations in the absorbance
176 intensity at specific bands. For example, pronounced increases with load were found
177 for peaks at 7003 cm^{-1} and 5220 cm^{-1}. The former was assigned to the first overtone of
178 the O–H stretching mode of the amorphous regions in cellulose and water.[42] The latter

179 was attributed to the combined O–H stretching and deformation modes in water.[42]
180 These results indicate that the NIR spectra vary mainly because of the densification of
181 the specimen.[43] The peak at 4808 cm^{-1}, which was attributed to the combined O–H
182 stretching and C–H deformation modes in the semi-crystalline or crystalline regions in
183 cellulose, gradually increased with load.[42] This also suggests the substantial changes of
184 molecules in the cell wall. Therefore, the spectral matrices presumably contained
185 information on both reversible and irreversible changes.

186 In this study, we examined the spectral variation based on statistical mechanics.
187 Therefore, we did not consider the spectral variation as an individual variable (i.e.,
188 wavenumber), but rather as a whole for the wood system. Statistical mechanics
189 consider the physical properties of systems consisting of an enormous number of
190 microscopic elements.[30,44,45] Here, we assumed that the spectral variables were
191 microscopic elements of the wood system. Therefore, rather than considering a single
192 dynamic system, we considered a collection of systems that correspond to the same
193 Hamiltonian, which is referred to as a statistical ensemble. A Gibbs ensemble of
194 systems can be represented by a point cloud in the *n*-dimensional phase space[17]; thus,
195 the NIR spectral matrix of an ensemble of wood samples can be identified with a point
196 cloud. Based on this suggestion, spectral variables function as generalized coordinates
197 in analytical mechanics.[36,37] In the following section, we discuss how the cloud flows,

changing its shape during the load-unload cycle, through the eigenvalue distribution.

For these reasons, many spectra that exhibited almost identical variation patterns were simulated based on bootstrap resampling.[46] Only 20 samples were collected, and 1,000 samples were simulated as follows[20]: the absorbance values for each wavenumber presumably obeyed the empirical distribution of the measured data, and the mean of the bootstrap samples was obtained repeatedly (1000 times) using the simpleboot package in R version 3.6.1.[47] Consequently, spectral matrices with 1000 rows and 1168 columns were obtained for each measurement point at times t_1, t_2, …, t_{60}; thus, we can examine the time evolution of the statistical ensemble.

3.3. Eigenvalue distribution

As an example, Figure 3 shows the trajectory of several eigenvalues during the loading and unloading process in the first cycle. While increasing the load level, the eigenvalues diffused without intersecting one another (Fig. 3(a)). Conversely, the distribution of eigenvalues decreased with unloading (Fig. 3(b)). These results were consistent with any cycle, indicating that the regularity of the NIR spectral variations changes with the load level. Therefore, the spectral matrix varies in a more orderly manner as the load increases.

As mentioned above, the set of eigenvalues can be identified using an energy function H, and the distribution function Z can be calculated as the summation of the

Boltzmann factor $\exp(-\beta\lambda_i)$. Then, the Helmholtz free energy F is defined as a function of β conditioned by the variance-covariance matrix $\boldsymbol{C}$: $F(\beta|\boldsymbol{C}) = -\beta^{-1}\log Z(\beta|\boldsymbol{C})$.[28–30] Based on the random matrix theory, the first eigenvalue λ_1 of matrix $\boldsymbol{C}$ can be evaluated by F in the limits of $\beta\to\infty$ as follows[26]:

$$\lambda_1 = 2\lim_{\beta\to\infty} F(\beta|\boldsymbol{C}). \quad (2)$$

Figure 4(a) shows the variation in λ_1 over five cycles. The red and blue lines correspond to the loading and unloading processes, respectively. The first eigenvalue λ_1 increased with load and decreased with unloading. Moreover, the convex changes in λ_1 during a single cycle gradually decreased as the cycle progressed. These results suggest that the Helmholtz free energy varied relative to the removal/application of load, and thus the amount of energy loss can be monitored directly as opposed to the area measurements from the load-displacement charts.

The randomness of the system can be evaluated from the eigenvalue distributions. Using the distribution function Z as a normalization factor, we calculated the probability of the system of interest to occupy the energy eigenstate i as follows[44,45]:

$$p_i^{\mathrm{can}} = \frac{1}{Z}\exp(-\beta\lambda_i). \quad (3)$$

The p_i^{can} is equivalent to a canonical distribution in statistical physics. Therefore, we can calculate the Shannon entropy S as a function of the probability p_i^{can} as follows[28]:

$$S = -\sum_{i=1}^{N} p_i^{\mathrm{can}} \log p_i^{\mathrm{can}} . \quad (4)$$

The inverse temperature β was set to be constant in this study ($\beta = 10^4$). As expected, the entropy S pattern was opposite to that of the Helmholtz free energy (Fig. 4(b)); in other words, S decreased with load and increased with unloading, and the concave changes in S during a single cycle gradually increased as the cycle progressed. These results imply that irreversible changes in wood gradually accumulate with an increase in the load-unload cycle.

Notably, the eigenvalue distribution method can evaluate the variation in the energy state of wood accompanying load/unloading in real time. In addition, NIR spectra contain microscopic information regarding molecules in the cell wall, as previously noted. All variations generated by the various chemical components in wood during the multiple cyclic processes were aggregated into a set of eigenvalues. Consequently, the eigenvalue distributions provide a macroscopic understanding of complex phenomena occurring at the microscopic scale via thermodynamic functions.

3.4. Evaluation of the irreversibility

As mentioned above, an ensemble of wood samples can be identified using a point cloud in an n-dimensional space. Suppose that the motion of a wood system with m points is expressed by the following Hamilton's equation:

$$\frac{dq_i}{dt} = \frac{\partial H}{\partial p_i}, \frac{dp_i}{dt} = \frac{\partial H}{\partial q_i}, \tag{5}$$

where $\boldsymbol{q} = (q_1, \cdots, q_n)$ represents the generalized coordinates and $\boldsymbol{p} = (p_1, \cdots, p_n)$ represents the momenta. A space with $2n$ dimensions spanned by q_1, …, p_n is termed the phase space. The point cloud can be described as a continuous fluid with a density of $\rho(q_1, \cdots, q_n, p_1, \cdots, p_n, t)$ in the phase space.[36,44] Based on quantum mechanics[23], the density matrix is calculated as follows:

$$\rho = \sum_{i=1}^{n} \boldsymbol{u}_i^{\mathrm{T}} p_i^{\mathrm{can}} \boldsymbol{u}_i, \tag{6}$$

where $\boldsymbol{u}_i$ (i = 1, …, n) is the eigenvector corresponding to eigenvalue λ_i, and the superscript notation T indicates the transposed matrix. The time evolution of the density matrix is given by the following Liouville-von Neumann equation[23,44]:

$$i\hbar \frac{\partial \rho}{\partial t} = [\rho, H], \tag{7}$$

where $i = \sqrt{-1}$ is an imaginary unit, $\hbar$ is the reduced Planck constant, H is the diagonal matrix whose elements are eigenvalues λ_1, λ_2, …, λ_N, and [,] is the commutator defined by two operators $[A, B] = AB - BA$. This can be interpreted as a volume change of fluid in the phase space.

Liouville's theorem states that the fluid volume in the phase space is invariant if the system satisfies the law of conservation.[36] Therefore, the density matrix ρ is the first integral of Hamilton's equation (5), determined by Hamiltonian H if and only if [ρ,

H] = 0. The right side of Eq. (7) was calculated for each cycle and was a non-zero matrix. Indeed, the matrix norms of commutator [ρ, H] for cycle 1, 2, 3, 4, and 5 were 5.72×10^{-6}, 5.25×10^{-6}, 5.30×10^{-6}, 4.93×10^{-6}, and 5.15×10^{-6}, respectively (Figure 5). Because energy invariance refers to the symmetry of a process from a geometrical perspective (Noether's theorem), the results infer that symmetry breakage during the cyclic process was greatest in the first cycle and decreased after the second cycle. Consequently, we conclude that *wood cannot be restored to its original state*. The load was easily restored during the cycle; however, even if the load returns to the initial point, not all other properties are restored to their original states.

4. Conclusion

This study proposed an algebraic approach to evaluate changes in the physical state of wood under multiple tensile load-unload cycles using NIR spectra. The NIR spectral matrix from a sample group was considered an operator representing the physical quantity of the statistical ensemble, and the set of eigenvalues calculated from the matrix was regarded as an energy function. Based on the distribution of eigenvalues accumulated for all microscopic changes, we monitored the variation of the energy state of wood in response to the load level. The commutator was defined by two operators, namely the density and diagonal matrix of the eigenvalues, and could quantitatively evaluate the irreversible changes of wood during the cyclic processes.

285 Considering that the eigenvalue distributions did not depend on a specific coordinate
286 system, the proposed method is suitable for multi-dimensional data other than that
287 obtained from the near-infrared spectrum.

CRediT authorship contribution statement

Takaaki Fujimoto: Investigation, formal analysis, resources, conceptualization, methodology, writing, review, and editing.

Declaration of competing interests

The author declares that they have no known competing financial interests or personal relationships that could have influenced the work reported in this study.

Acknowledgements

The author acknowledges Professor Satoru Tsuchikawa of Nagoya University for assisting with NIR measurements. I am also grateful to Mr. Shogo Fukutomi and Ms. Asami Yoneda of the Tottori University Forest for harvesting the sample trees. This work was supported by JSPS KAKENHI (grant number: JP21K05709). I would like to thank Editage (www.editage.com) for the English language editing.

References

1. Čermák P, Vahtikari K, Rautkari L, Laine K, Horáček P and Baar J. The effect of wetting cycles on moisture behaviour of thermally modified Scots pine (*Pinus sylvestris* L.) wood. *J Mater Sci* 2016; 51: 1504–1511.
2. Gunjal J, Abhilash RM and Chauhan SS. Effect of repeated cycles of wetting and drying on mechanical properties of wood–polypropylene composites. *J Indian Acad Wood Sci* 2020; 17: 114–122.
3. Obataya E and Higashihara T. 2017. Reversible and irreversible dimensional changes of heat-treated wood during alternate wetting and drying. *Wood Sci Technol* 2017; 51: 739–749.
4. Bodig J and Jayne BA. *Mechanics of Wood and Wood Composites*. Melbourne, Florida: Krieger Publishing Company, 1993.
5. Gaff M and Gáborík J. Effect of cyclic loading on the elasticity of beech solid and laminated wood. *BioResources* 2014; 9: 4288–4296.
6. Stanciu MD, Teodorescu HD and Vlase S. Degradation of mechanical properties of pine wood under symmetric axial cyclic loading parallel to grain. *Polymers* 2020; 12: 2176.
7. Cavallaro G, Lazzara G, Milioto S, Parisi F and Sparacino V. Thermal and dynamic mechanical properties of beeswax-halloysite nanocomposites for consolidating

waterlogged archaeological woods. *Polym Degrad Stab* 2015; 120: 220–225.

8. Inagaki T, Yonenobu H and Tsuchikawa S. Near-infrared spectroscopic monitoring of the water adsorption/desorption process in modern and archaeological wood. *Appl Spectrosc* 2008; 62: 860–865.
9. Riggio M, Sandak J, Sandak A, Pauliny D and Babiński L. Analysis and prediction of selected mechanical/dynamic properties of wood after short and long-term waterlogging. *Constr Build Mater* 2014; 68: 444–454.
10. Keckes J, Burgert I, Frühmann K, Müller M, Kölln K, Hamilton M, Burghammer M, Roth SV, Stanzl-Tschegg S and Fratzl P. Cell-wall recovery after irreversible deformation of wood. *Nat Mater* 2003; 2: 810–814.
11. Montero C, Clair B, Alméras T, van der Lee A and Gril J. Relationship between wood elastic strain under bending and cellulose crystal strain. *Compos Sci Technol* 2012; 72: 175–181.
12. Nakai T, Yamamoto H and Nakao T. The relationship between macroscopic strain and crystal lattice strain in wood under uniaxial stress in the fiber direction. *J Wood Sci* 2005; 51: 193–194.
13. Toba K, Yamamoto H and Yoshida M. Mechanical interaction between cellulose microfibrils and matrix substances in wood cell walls induced by repeated wet-and-dry treatment. *Cellulose* 2021; 19: 1405–1412.

14. Dinwoodie JM. *Timber: Its Nature and Behaviour*. Second ed. London: E. and F. N. Spon, 2000.

15. Majka J, Czajkowski Ł and Olek W. Effects of cyclic changes in relative humidity on the sorption hysteresis of thermally modified spruce wood. *BioResources* 2016; 11: 5265–5275.

16. Patera A, Derome D, Griffa M and Carmeliet J. Hysteresis in swelling and in sorption of wood tissue. *J Struct Biol* 2013; 182: 226–234.

17. Prigogine I. *From Being to Becoming – Time and Complexity in the Physical Sciences*. San Francisco: W. H. Freeman and Company, 1980.

18. Zobel BJ and van Buijtenen JP. *Wood Variation – Its Causes and Control*. Berlin Heidelberg New York: Springer, 1989.

19. Fujimoto T. Evaluation of wood variation based on the eigenvalue distribution of near infrared spectral matrix. *J Near Infrared Spectrosc* 2019; 27: 175–180.

20. Fujimoto T. Evaluation of stress relaxation process of wood based on the eigenvalue distribution of near infrared spectra. *Spectrochim Acta A Mol Biomol Spectrosc* 2021; 248: 119197.

21. Tsutsumi H, Haga H and Fujimoto T. Variation in wood shrinkage evaluated by the eigenvalue distribution of the near infrared spectral matrix. *Vib Spectrosc* 2020; 109: 103091.

22. Tsutsumi H, Haga H and Fujimoto T. Energetics of the distribution of cell wall in wood based on an eigenvalue analysis. *J Wood Sci* 2020; 66: 58.

23. Schwabl F. *Quantum Mechanics*. Fourth ed. Berlin Heidelberg: Springer-Verlag, 2007.

24. Dyson FJ. A Brownian-motion model for the eigenvalues of a random matrix. *J Math Phys* 1962; 3: 1191–1198.

25. Dyson FJ. Statistical theory of the energy levels of complex systems I. *J Math Phys* 1962; 3: 140–156.

26. Kabashima Y and Takahashi H. First eigenvalue/eigenvector in sparse random symmetric matrices: influences of degree fluctuation. *J Phys A: Math Theor* 2012; 45: 325001.

27. Mehta ML. *Random Matrices*. Third ed. London: Elsevier Ltd, 2004.

28. Helrich CS. *Modern Thermodynamics with Statistical Mechanics*. Berlin Heidelberg: Springer-Verlag, 2009.

29. Landau DP and Binder K. *A Guide to Monte Carlo Simulations in Statistical Physics*. Fourth ed. Cambridge: Cambridge University Press, 2015.

30. Schwabl F. *Statistical Mechanics*. Second ed. Berlin Heidelberg: Springer-Verlag, 2006.

31. Tsuchikawa S. A review of recent near infrared research for wood and paper. *Appl*

Spectrosc Rev 2007; 42: 43–71.

32. Tsuchikawa S and Schwanninger M. A review of recent near infrared research for wood and paper. Part 2. *Appl Spectrosc Rev* 2013; 48: 560–587.
33. Tsuchikawa S and Kobori H. A review of recent application of near infrared spectroscopy to wood science and technology. *J Wood Sci* 2015; 61: 213–220.
34. Tsutsumi H, Oribe S, Haga H and Fujimoto T. Nondestructive evaluation of wood properties in standing trees using vibrational spectra. *Mokuzai Gakkaishi* 2017; 63: 291–296.
35. Tu LW. *An Introduction to Manifolds*. New York: Springer Science+Business Media Inc, 2008.
36. Arnold VI. *Mathematical Methods of Classical Mechanics*. Second ed. New York: Springer Science+Business Media Inc, 1989.
37. Lanczos C. *The Variational Principles of Mechanics*. Fourth ed. New York: Dover Publications Inc, 1970.
38. Lang S. *Linear Algebra*. Third ed. New York: Springer Science+Business Media Inc, 1987.
39. Hoyle DC and Rattray M. Principal-component-analysis eigenvalue spectra from data with symmetry-breaking structure. *Phys Rev E* 2004; 69: 026124.
40. Newman RH, Battley MA, Carpenter JEP and Le Guen MJ. Energy loss in a

unidirectional flax-polyester composite subjected to multiple tensile load–unload cycles. *J Mater Sci* 2012; 47: 1164–1170.

41. Fantozzi G and Reynaud P. Mechanical hysteresis in ceramic matrix composites. *Mater Sci Eng A* 2009; 521–522: 18–23.
42. Schwanninger M, Rodrigues JC and Fackler K. A review of band assignments in near infrared spectra of wood and wood components. *J Near Infrared Spectrosc* 2011; 19: 287–308.
43. Fujimoto T, Kobori H and Tsuchikawa S. Prediction of wood density independently of moisture conditions using near infrared spectroscopy. *J Near Infrared Spectrosc* 2012; 20: 353–359.
44. Toda M, Kubo R and Saito N. *Statistical physics I. Equilibrium Statistical Mechanics*. Third corrected printing. Berlin Heidelberg: Springer-Verlag, 1998.
45. Kubo R, Toda M and Hashitsume N. *Statistical physics II. Nonequilibrium Statistical Mechanics*. Third corrected printing. Berlin Heidelberg: Springer-Verlag, 1998.
46. Efron B and Tibshirani RJ. *An Introduction to the Bootstrap*. New York: Chapman & Hall, 1993.
47. Peng RD. Package 'simpleboot': simple bootstrap Routines. R package version 1.1-7, 2019. https://cran.r-project.org/web/packages/simpleboot/simpleboot.pdf.

Figure Captions

Figure 1. Load-displacement curves during the cyclic tensile test. The red and blue lines indicate the loading and unloading process, respectively. The color becomes lighter as the cycles increase.

Figure 2. Variation of the diffuse reflectance NIR spectra obtained from (a) the loading and (b) unloading process. The color of the spectra changes from yellow to red (or blue) as the process progresses.

Figure 3. Trajectory of representative eigenvalues during (a) the loading and (b) unloading process. The results of the first cycle are shown as an example.

Figure 4. Variation of (a) the first eigenvalue and (b) entropy over the five cycles. The red and blue lines indicate the loading and unloading process, respectively. The gray lines indicate the mean value of the first eigenvalue and entropy in each cycle.

Figure 5. Matrix norms of commutator [ρ, H] for each cycle.

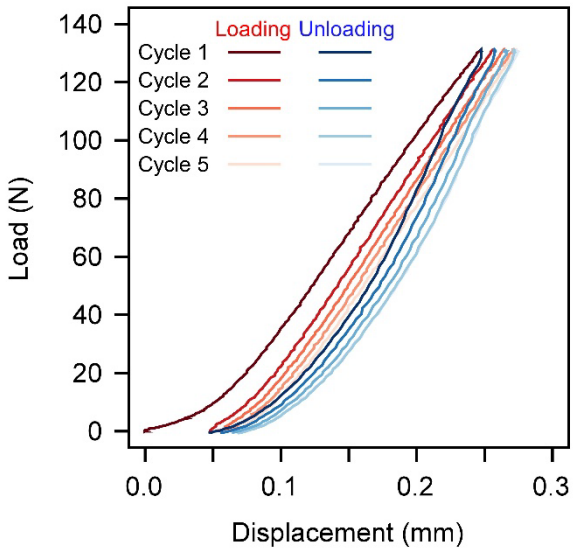
Loading Unloading
Cycle 1
Cycle 2
Cycle 3
Cycle 4
Cycle 5
Load (N)
140
120
100
80
60
40
20
0
0.0
0.1
0.2
0.3
Displacement (mm)

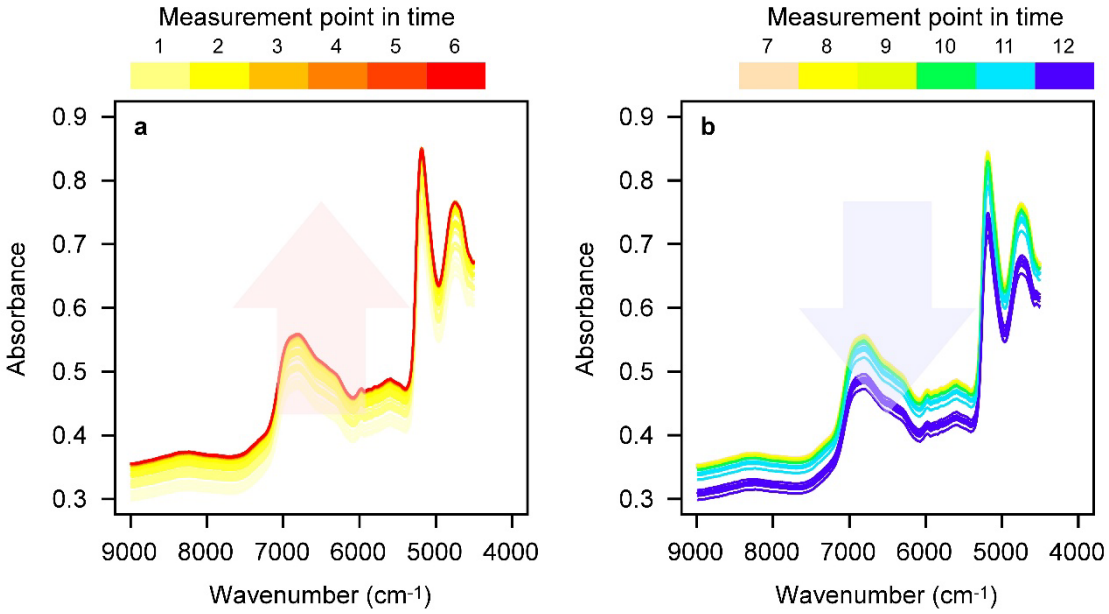
Measurement point in time
1 2 3 4 5 6
a
Absorbance
0.9
0.8
0.7
0.6
0.5
0.4
0.3
9000 8000 7000 6000 5000 4000
Wavenumber (cm-1)
Measurement point in time
7 8 9 10 11 12
b
Absorbance
0.9
0.8
0.7
0.6
0.5
0.4
0.3
9000 8000 7000 6000 5000 4000
Wavenumber (cm-1)

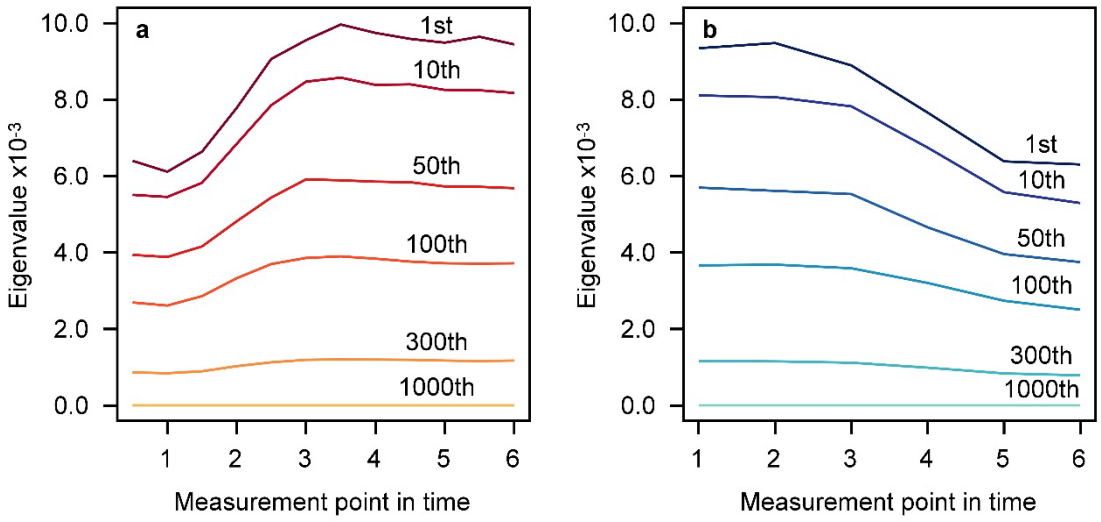
a
b
1st
10th
50th
100th
300th
1000th
Eigenvalue x10-3
10.0
8.0
6.0
4.0
2.0
0.0
1
2
3
4
5
6
Measurement point in time

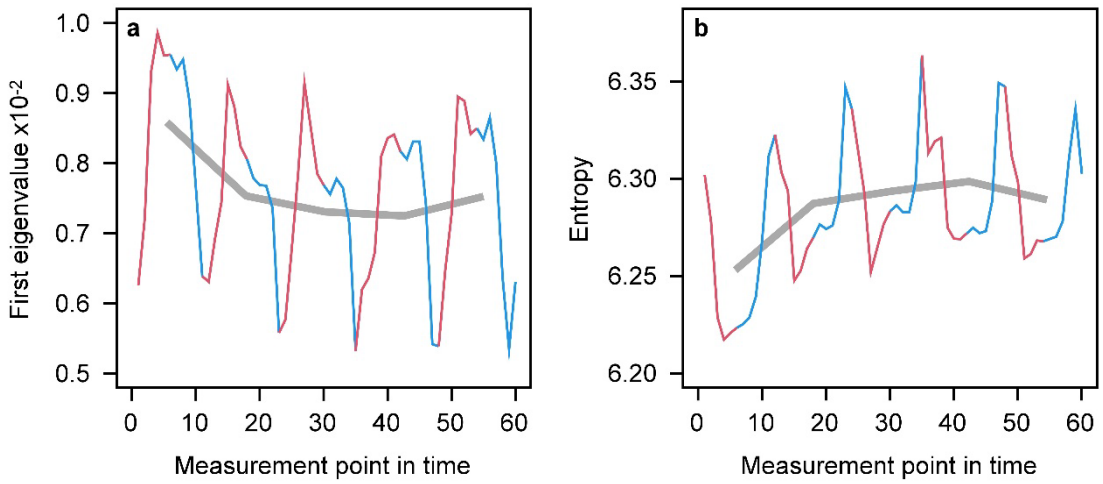
a
First eigenvalue x10-2
1.0
0.9
0.8
0.7
0.6
0.5
0
10
20
30
40
50
60
Measurement point in time
b
Entropy
6.35
6.30
6.25
6.20
0
10
20
30
40
50
60
Measurement point in time

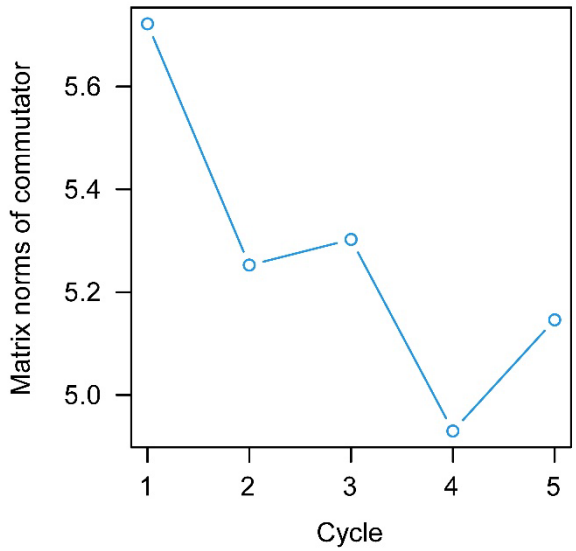
Matrix norms of commutator
5.6
5.4
5.2
5.0
1
2
3
4
5
Cycle